Influence of sustained stress on the durability of glass FRP reinforcing bars

T. D'Antino *, M.A. Pisani

Department of Architecture, Built Environment and Construction Engineering, Politecnico di Milano, Piazza Leonardo da Vinci 32, 20133 Milan, Italy

Glass fiber reinforced polymer (GFRP) bars can be employed as an alternative to steel bars for internal reinforcement of concrete elements. Although GFRP bars have been used to reinforce concrete for the last two decades, their long-term behavior is still an open issue. The tensile strength of bars subjected to aggressive exposure conditions has been investigated by different authors. However, clear and reliable indications on the bar residual strength are still lacking. Furthermore, the effect of sustained stress on the bar tensile strength is not completely clear and severe limitations on the stress level attained by the bar are imposed by available design guidelines.

In this paper, the effect of sustained stress on GFRP bars exposed to different environmental conditions, namely air, alkaline environments, deionized water, and salt solutions, is studied by analyzing a database comprising 127 GFRP bar tensile tests collected from the literature. The results are analyzed and discussed to investigate the effect of sustained stress on the tensile strength of GFRP bars and to calibrate characteristic and design values for tensile strength long-term reduction factors.

Highlights

- Tensile test results on conditioned GFRP bars were collected from the literature.
- Bars were subjected to contemporary sustained stress and aggressive environment.
- The sustained stress had a limited influence on the bar residual tensile strength.
- Characteristic and design reduction factors for long-term behavior were calibrated.

Keywords: GFRP bars, Long-term behavior, Sustained stress, Design values

1. Introduction

All materials exhibit weaknesses related to specific environmental conditions. In particular, steel can be damaged by corrosion, which in reinforced concrete (RC) elements reduces the resisting cross-section and causes cracking and spalling of concrete with consequent need of expensive retrofitting. Fiber reinforced composites represent a possible solution for strengthening deteriorated existing concrete and masonry structures [1–7]. Furthermore, Glass Fiber Reinforced Polymer (GFRP) bars can be adopted for internal reinforcement of new concrete elements as an alternative to traditional steel rebar in aggressive environmental conditions and especially for elements exposed to salt water environments [8–11]. As a matter of fact, hulls of boats have been made of fiberglass for the last half of a century [12].

Article history:
Received 12 April 2018
Received in revised form 20 July 2018
Accepted 24 July 2018

* Corresponding author.
E-mail address: tommaso.dantino@polimi.it (T. D'Antino).

However, GFRP reinforcing bars present some weaknesses. Between them, the most important is the glass fiber sensitiveness to high-alkalinity environments, such as concrete. Indeed, in concrete elements the alkalinity is generally kept high to protect the steel reinforcement from corrosion and the presence of moisture contributes to the increase of the pH. Furthermore, GFRP bars may be damaged by exposure to relatively high temperatures (because of the degradation of the organic matrix properties) and to water that affects the mechanical behavior of the glass fibers [13–16].

Depending on the type of matrix used and on the environment, moisture (or alkaline solution) diffuses into the polymer matrix for varying extents and at various rates, eventually reaching the glass fibers and deteriorating them through a diffusion process that occurs at the molecular level [17].

In addition to being exposed to moisture and to an alkaline environment, GFRP reinforcing bars are subjected to sustained (permanent and quasi-permanent) stresses. If these stresses

Published Journal Article available at https://doi.org/10.1016/j.conbuildmat.2018.07.175

induce cracks in the polymer matrix, moisture can reach the glass fibers with a rate higher than that associated with the diffusion process. Therefore, the level of sustained stress shall be taken into account to assess the residual strength of GFRP reinforcing bars subjected to aggressive environments.

Some experimental studies have been carried out to find a correlation between the bar residual strength, type of environment, and level of sustained load (e.g. [18]). However, results are often contradictory and a clear understanding of this relation is still missing in the available scientific literature.

In this paper, 127 experimental GFRP bar tensile tests found in the literature, performed by 8 different research groups, were analyzed trying to provide a clear insight on the effect of sustained stress on the residual strength of GFRP bars. Different parameters, such as the exposure temperature, sustained load duration, and sustained stress ratio were analyzed. Furthermore, the results of tensile tests on 47 bars conditioned in alkaline environments and with the simultaneous application of a sustained stress were compared with 178 results of tensile tests of stress-free GFRP bars exposed to alkaline environments to study the effect of sustained stress on the bar residual strength.

2. Experimental database

The results of 127 tensile tests of GFRP bars exposed to air and to different aggressive environments while a sustained tensile stress was applied, reported in eight different research studies, were collected from the literature [18–25]. All tests collected were carried out using a tensile test set-up where the bar ends were embedded within metallic tubes to avoid possible stress concentrations and attain the complete bar failure [11]. Results of tensile tests that did not report a complete bar failure were disregarded. The tensile stress ratio applied to the specimens σ_S/σ_{fu}, which is defined as the ratio between the sustained stress σ_S and the tensile strength of the corresponding unconditioned (control) specimen σ_{fu}, varies between 10% and 80% for the bars included in the database. Furthermore, the bars considered present different fiber volume fraction v_f, which is defined as the ratio between the fiber volume and volume of the bar and ranges between 45% and 76%, diameter ϕ, ranging between 9.0 mm and 16.0 mm, and tensile strength σ_{fu}, ranging between 532 MPa and 1410 MPa. The surface of the specimens was treated in different ways, namely ribbed (R), sand coated (Sa), helically wrapped (W), grooved (G), or a combination of these. The matrices employed were vinylester (VE), polyester (PE), urethane modified vinylester (UM-VE), mixed vinylester and polyethylene terephthalate (V-PET), or mixed vinylester and polyester (VE + PE). Six bars were made of alkali-resistant (AR) glass fibers, whereas the remaining bars were made of E-glass (E) fibers. Details of each specimen are reported in Table 1, whereas the frequency distribution of sustained stress ratio σ_S/σ_{fu}, fiber volume fraction v_f, diameter ϕ, and unconditioned tensile strength σ_{fu} of bars included in the database are reported in Fig. 1a, b, c, and d, respectively. The residual strength ratio, σ_f/σ_{fu}, defined as the ratio between the tensile strength of the conditioned specimen σ_f and the corresponding σ_{fu} value, and the time (duration) of simultaneous environmental and sustained stress exposure are also reported in Table 1 for each specimen.

3. Analysis of the results

In this section, the results of tensile tests on GFRP bars collected from the literature are analyzed to shed light on the effect of simultaneous sustained stress and exposure to:

I. air (laboratory conditions);
II. alkaline solution;
III. deionized water;
IV. salt solutions.

In addition, a comparison between the results of bars exposed to alkaline solutions with and without the application of a sustained stress is shown and discussed. Results are compared in terms of residual strength ratio, σ_f/σ_{fu}, (see Table 1). The effect of exposure temperature, sustained load duration, and sustained stress ratio are investigated. The fiber volume fraction was not considered between parameters studied because previous work showed that v_f had a limited influence of the residual strength ratio obtained [26].

3.1. Bars exposed to air (laboratory conditions)

Two research groups studied the effect of sustained stress levels on GFRP bars exposed to laboratory environmental conditions. Sustained stress ratios between 10.5% and 80% were applied to 51 bars for 1440 and 10,000 h. The residual strength ratios obtained, which are depicted in Fig. 2a and b with respect to the sustained stress duration and sustained stress ratio, respectively, show that the bar tensile properties were not affected by the sustained stress application. The average residual strength ratio of specimens in Fig. 2 is 98.98% (coefficient of variation CoV = 0.032), which demonstrates that in absence of an aggressive environment the cracks and microcracks possibly caused by the sustained stress did not affect σ_f/σ_{fu}.

3.2. Bars subjected to alkaline environment

Forty-seven GFRP bars, tested by six research groups, were subjected to different sustained stress ratios and exposed to alkaline environments for exposure time between 720 and 10,008 h. Sixteen bars were embedded within concrete prisms and cylinders that were kept moist in the same water employed for curing. The bars were extracted from concrete just before performing the tensile tests [21,24]. Seven bars were immersed in a solution that simulates the alkalinity of concrete pore water (“Pore water” in Table 1). Forty-one bars were made of E-glass fibers whereas 6 bars comprised AR-glass fibers (indicated with AR in Fig. 3 legend and in the remaining of the paper). Specimens tested by Vijay [25] and exposed to an alkaline solution with freeze and thaw cycles were not considered in the analysis. Since various exposure temperatures were employed to accelerate the alkali degradation, specimens were divided in three temperature ranges, namely 22–23 °C, 40–55 °C, and 56–65 °C. The pH of the conditioning environment varied from author to author within the range $10.5 \leq pH \leq 13.1$. The influence of the solution alkalinity was not investigated in this section. An investigation of the effect of different alkaline solutions on the residual strength of GFRP bars can be found in Ref. [26]. Since bars comprised of AR-glass showed residual strength ratios similar to those of E-glass bars with the same characteristic, AR-glass bars were also considered in this section.

The residual strength ratio obtained for each bar with respect to the sustained stress duration and to the sustained stress ratio are depicted in Fig. 3a and b, respectively. To study what parameters affect the residual strength ratio, the exposure temperature, sustained stress duration, and sustained stress ratio should be considered at the same time. The results show that the exposure temperature did not have a clear influence on the residual strength ratio. Although specimens conditioned for the same exposure time and with the same sustained stress ratio showed a reduction of σ_f/σ_{fu} for increasing exposure temperature (see also Table 1), slight differences of the exposure time led to significant variation of σ_f/σ_{fu}, which suggests that various parameters may have affected the results. The testing procedure is one of the main

Table 1
Database of GFRP bars exposed to aggressive environment and with applied sustained stress.

R	Fiber type	v_f [%]	Matrix type	ϕ [mm]	σ_{fu} [MPa]	Surface	Environmental conditions	pH	Temp [°C]	Time [h]	σ_s/σ_{fu} [%]	σ_f/σ_{fu} [%]
[19]	E	57	VE	9.5	854	Sa	Air		23.0	10,000	12.4	101.0
	E	57	VE	9.5	854	Sa	Air		23.0	10,000	12.4	101.3
	E	57	VE	9.5	854	Sa	Air		23.0	10,000	14.4	100.4
	E	57	VE	9.5	854	Sa	Air		23.0	10,000	12.6	101.3
	E	57	VE	9.5	854	Sa	Air		23.0	10,000	14.8	98.9
	E	51	VE	9.5	828	Wsa	Air		23.0	10,000	11.0	99.9
	E	51	VE	9.5	828	Wsa	Air		23.0	10,000	10.5	101.9
	E	65	VE	12.7	774	Sa	Air		23.0	10,000	16.2	102.3
	E	65	VE	12.7	774	Sa	Air		23.0	10,000	16.2	100.8
	E	65	VE	12.7	774	Sa	Air		23.0	10,000	14.8	100.4
	E	65	VE	12.7	774	Sa	Air		23.0	10,000	16.0	103.5
	E	75	VE	12.0	1410	G	Air		23.0	10,000	13.4	97.6
	E	75	VE	12.0	1410	G	Air		23.0	10,000	12.9	101.4
	E	75	VE	12.0	1410	G	Air		23.0	10,000	16.0	97.5
	E	75	VE	12.0	1410	G	Air		23.0	10,000	13.0	96.9
	E	67	VE	15.9	748	Sa	Air		23.0	10,000	14.1	95.6
	E	67	VE	15.9	748	Sa	Air		23.0	10,000	15.7	95.1
	E	67	VE	15.9	748	Sa	Air		23.0	10,000	15.4	93.9
	E	67	VE	15.9	748	Sa	Air		23.0	10,000	14.1	96.4
	E	58	VE	15.9	783	Wsa	Air		23.0	10,000	14.8	102.0
	E	58	VE	15.9	783	Wsa	Air		23.0	10,000	19.0	102.3
	E	58	VE	15.9	783	Wsa	Air		23.0	10,000	17.1	97.3
	E	57	VE	9.5	854	Sa	Air		23.0	10,000	31.1	97.1
	E	57	VE	9.5	854	Sa	Air		23.0	10,000	28.6	101.0
	E	57	VE	9.5	854	Sa	Air		23.0	10,000	33.0	95.0
	E	57	VE	9.5	854	Sa	Air		23.0	10,000	28.8	95.5
	E	51	VE	9.5	828	Wsa	Air		23.0	10,000	37.6	104.4
	E	51	VE	9.5	828	Wsa	Air		23.0	10,000	29.1	97.4
	E	51	VE	9.5	828	Wsa	Air		23.0	10,000	48.7	92.4
	E	51	VE	9.5	828	Wsa	Air		23.0	10,000	30.3	94.1
	E	65	VE	12.7	774	Sa	Air		23.0	10,000	24.3	103.6
	E	65	VE	12.7	774	Sa	Air		23.0	10,000	25.9	99.1
	E	65	VE	12.7	774	Sa	Air		23.0	10,000	29.1	102.5
	E	65	VE	12.7	774	Sa	Air		23.0	10,000	26.5	97.0
	E	65	VE	12.7	774	Sa	Air		23.0	10,000	24.6	104.7
	E	65	VE	12.7	774	Sa	Air		23.0	10,000	25.6	98.3
	E	75	VE	12.0	1410	G	Air		23.0	10,000	20.3	97.0
	E	75	VE	12.0	1410	G	Air		23.0	10,000	20.0	96.9
	E	75	VE	12.0	1410	G	Air		23.0	10,000	17.2	96.6
	E	75	VE	12.0	1410	G	Air		23.0	10,000	18.8	98.9
	E	67	VE	15.9	748	Sa	Air		23.0	10,000	37.3	94.3
	E	67	VE	15.9	748	Sa	Air		23.0	10,000	30.9	97.9
	E	67	VE	15.9	748	Sa	Air		23.0	10,000	29.1	94.0
	E	58	VE	15.9	783	Wsa	Air		23.0	10,000	32.8	104.9
	E	58	VE	15.9	783	Wsa	Air		23.0	10,000	26.2	100.1
	E	58	VE	15.9	783	Wsa	Air		23.0	10,000	30.1	99.2
[20]	E	66	VE	12.7	854	Sa	Air		23.0	1440	80.0	103.0
	E	66	VE	12.7	854	Sa	Air		23.0	1440	80.0	97.2
	E	66	VE	12.7	854	Sa	Air		23.0	1440	80.0	99.8
	E	66	VE	12.7	854	Sa	Air		23.0	1440	80.0	97.8
	E	66	VE	12.7	854	Sa	Air		23.0	1440	80.0	100.7
[21]	E	75	VE + PE	12.4	702	W	Pore water	12.8	22	2160	30.0	84.8
	E	75	VE + PE	12.4	634	W	Pore water	12.8	22	2160	30.0	85.6
	AR	75	VE + PE	9.3	617	W	Pore water	12.8	22	3360	30.0	101.2
	AR	75	VE + PE	9.3	617	W	Concrete	10.5	22	3360	30.0	100.6
	AR	75	PE	9.3	650	W	Pore water	12.8	22	3360	30.0	95.1
	AR	75	PE	9.3	650	W	Concrete	10.5	22	3360	30.0	101.5
	E	75	VE	12.4	612	W	Pore water	12.8	22	2160	30.0	96.0
	AR	75	VE	9.3	532	W	Pore water	12.8	22	3360	30.0	101.0
	E	75	VE	9.3	958	W	Pore water	12.8	22	3360	30.0	83.3
	AR	75	VE	9.3	532	W	Concrete	10.5	22	3360	30.0	98.8
	E	75	VE	9.3	958	W	Concrete	10.5	22	3360	30.0	83.9
	E	68	V-PET	12.0	693	R	Alk sol	12.1	22	720	30.0	94.0
	E	68	V-PET	12.0	693	R	Alk sol	13.1	22	720	30.0	94.0
	E	68	V-PET	12.0	693	R	Alk sol	12.1	22	720	60.0	100.0
	E	68	V-PET	12.0	693	R	Alk sol	13.1	22	720	60.0	78.0
[22]	E	73	VE	12.7	639		DI water	7.0	63	2496	29.0	73.0
	E	73	VE	12.7	639		DI water	7.0	62	2496	21.0	89.0
	E	73	VE	12.7	639		DI water	7.0	61	2496	20.0	76.0
	E	73	VE	12.7	639		DI water	7.0	60	2496	20.0	82.0
	E	73	VE	12.7	639		DI water	7.0	60	2496	20.0	85.0
	E	73	VE	12.7	639		DI water	7.0	60	2496	27.0	79.0

Table 1 (*continued*)

R	Fiber type	v_f [%]	Matrix type	ϕ [mm]	σ_{fu} [MPa]	Surface	Environmental conditions	pH	Temp [°C]	Time [*h*]	σ_s/σ_{fu} [%]	σ_f/σ_{fu} [%]
	E	73	VE	12.7	639		DI water	7.0	57	2496	23.0	93.0
	E	73	VE	12.7	639		DI water	7.0	56	2496	20.0	98.0
	E	73	VE	12.7	639		Alk sol	12.9	62	2496	21.0	75.0
	E	73	VE	12.7	639		Alk sol	12.9	61	2496	18.0	81.0
	E	73	VE	12.7	639		Alk sol	12.9	61	2496	20.0	85.0
	E	73	VE	12.7	639		Alk sol	12.9	51	2496	24.0	84.0
	E	73	VE	12.7	639		Alk sol	12.9	49	2496	22.0	86.0
	E	73	VE	12.7	639		Alk sol	12.9	46	2496	20.0	87.0
	E	73	VE	12.7	639		Alk sol	12.9	45	2496	24.0	82.0
[18]	E	75	VE	9.5	658	Sa	DI water	7.0	23	10,000	25.0	92.7
	E	75	VE	9.5	658	Sa	DI water	7.0	23	10,000	38.0	96.2
	E	75	VE	9.5	658	Sa	Alk sol	12.8	23	10,000	29.0	84.4
	E	75	VE	9.5	658	Sa	Alk sol	12.8	23	10,000	38.0	65.1
[23]	E	75	VE	16	580	Sa	DI water	7.0	58	720	25.0	96.0
	E	75	VE	16	580	Sa	DI water	7.0	60	1440	25.0	90.0
	E	75	VE	9.5	580	Sa	DI water	7.0	72	1440	25.0	96.0
	E	75	VE	12.7	580	Sa	DI water	7.0	60	2880	25.0	85.0
	E	75	VE	9.5	580	Sa	DI water	7.0	23	10,008	25.0	92.7
	E	75	VE	16.0	580	Sa	Alk sol	12.8	55	720	25.0	98.0
	E	75	VE	16.0	580	Sa	Alk sol	12.8	61	1440	25.0	84.0
	E	75	VE	9.5	580	Sa	Alk sol	12.8	64	1440	25.0	88.0
	E	75	VE	12.7	580	Sa	Alk sol	12.8	57	2880	25.0	83.0
	E	75	VE	9.5	580	Sa	Alk sol	12.8	23	10,008	25.0	84.4
[24]	E	65.5	VE	12.7	854	Sa	Concrete		23	1440	80.0	99.1
	E	65.5	VE	12.7	854	Sa	Concrete		23	2880	80.0	99.4
	E	65.5	VE	12.7	854	Sa	Concrete		23	4320	80.0	97.9
	E	65.5	VE	12.7	854	Sa	Concrete		23	5760	80.0	94.8
	E	65.5	VE	12.7	854	Sa	Concrete		40	1440	80.0	99.2
	E	65.5	VE	12.7	854	Sa	Concrete		40	2880	80.0	97.4
	E	65.5	VE	12.7	854	Sa	Concrete		40	4320	80.0	96.4
	E	65.5	VE	12.7	854	Sa	Concrete		40	5760	80.0	91.8
	E	65.5	VE	12.7	854	Sa	Concrete		50	1440	80.0	98.1
	E	65.5	VE	12.7	854	Sa	Concrete		50	2880	80.0	98.0
	E	65.5	VE	12.7	854	Sa	Concrete		50	4320	80.0	94.6
	E	65.5	VE	12.7	854	Sa	Concrete		50	5760	80.0	89.9
[25]	E	45	UM-VE	12.7	606	Sa	Salt	7.0	23	2160	38.0	77.4
	E	45	UM-VE	12.7	609	R	Salt	7.0	23	2160	31.0	88.6
	E	45	UM-VE	12.7	606	Sa	Salt	7.0	23	5760	27.0	77.1
	E	45	UM-VE	12.7	606	Sa	Salt	7.0	23	8640	19.0	80.7
	E	45	UM-VE	12.7	609	R	Salt	7.0	23	4320	27.0	86.6
	E	45	UM-VE	12.7	609	R	Salt	7.0	23	7200	32.0	74.8
	E	45	UM-VE	12.7	606	Sa	Salt + FT	7.0	−18/+21	2160	22.0	96.7
	E	45	UM-VE	12.7	606	Sa	Salt + FT	7.0	−18/+21	4320	30.0	86.4
	E	45	UM-VE	12.7	606	Sa	Salt + FT	7.0	−18/+21	8640	30.0	96.8
	E	45	UM-VE	12.7	606	Sa	Salt + FT	7.0	-18/+21	8640	35.0	74.4
	E	45	UM-VE	12.7	606	Sa	Alk sol	13.0	23	4320	37.0	50.8
	E	45	UM-VE	12.7	606	Sa	Alk sol	13.0	23	5760	25.0	60.5
	E	45	UM-VE	12.7	609	R	Alk sol	13.0	23	4320	30.0	89.7
	E	45	UM-VE	12.7	609	R	Alk sol	13.0	23	5760	25.0	85.8
	E	45	UM-VE	12.7	606	Sa	Alk sol	13.0	23	8640	24.0	58.1
	E	45	UM-VE	12.7	606	Sa	Alk sol	13.0	23	8640	15.0	83.4
	E	45	UM-VE	12.7	606	Sa	Alk sol + FT	13.0	23	4320	33.0	53.3
	E	45	UM-VE	12.7	606	Sa	Alk sol + FT	13.0	23	5760	39.0	29.0
	E	45	UM-VE	12.7	606	Sa	Alk sol + FT	13.0	23	8640	30.0	40.7
	E	45	UM-VE	12.7	606	Sa	Alk sol + FT	13.0	23	8640	49.0	17.9

Note: R = reference; Fiber type: AR = alkali-resistant, E = E-glass; Matrix Type: VE = vinylester, PE = polyester, UM-VE = urethane modified vinylester, V-PET = mixed vinylester and polyethylene terephthalate, VE + PE = mixed vinylester and polyester; Surface: R = ribbed, Sa = sand coated, W = helically wrapped, Wsa = W + Sa, G = grooved; Environmental conditions: Alk sol = alkaline solution, DI = deionized, FT = freeze-thaw cycles.

parameters that affect the failure mode and, consequently, the result obtained. Due to the orthotropy of GFRP bars, a gripping method able to transfer the tensile stress to the testing machine without damage of the bar shall be employed. Depending on the gripping method adopted, different failure modes can be attained, namely i) complete tensile rupture of the bar, ii) slippage at the bar-anchor head interface, iii) fiber trimming on the collar of the anchor area, and iv) bar longitudinal delamination [26]. The GFRP bar tensile strength is attained only with complete tensile rupture of the bar, whereas other failure modes provide an underestimation of the bar tensile strength. Therefore, a detailed description of the bar failure mode should be always provided and results from specimens that reported different failure modes should be carefully compared [26].

Fig. 3b shows that the stress ratio adopted had no influence on the residual strength ratio. In fact, specimens subjected to σ_s/σ_{fu} = 20% and 80% at 40–55 °C tested by Debaiky et al. [23] and Robert et al. [24] showed similar values of σ_f/σ_{fu}. Analogously, Benmokrane et al. [21] obtained similar residual strength ratios for specimens subjected to σ_s/σ_{fu} = 30% and 60% for the same exposure time (720 h). The lowest residual strength ratios were obtained by Nkurunziza et al. [18] and Vijay [25] for sustained stress duration between 4320 and 10,000 h and for sustained stress ratios between 24% and 38%. These results are not consistent with

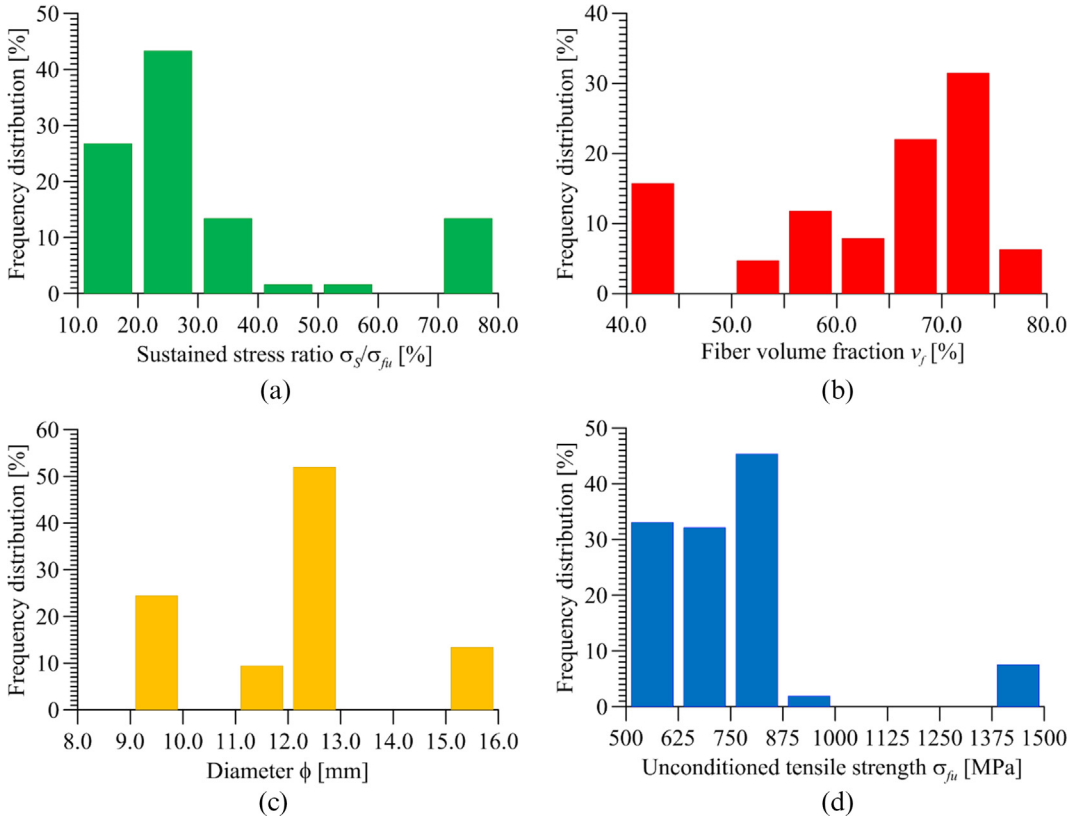

Fig. 1. Frequency distribution of a) sustained stress ratio $\sigma_S/\sigma_{fu,}$ b) fiber volume fraction v_f, c) diameter ϕ, and d) unconditioned tensile strength σ_{fu} of bars included in the database.

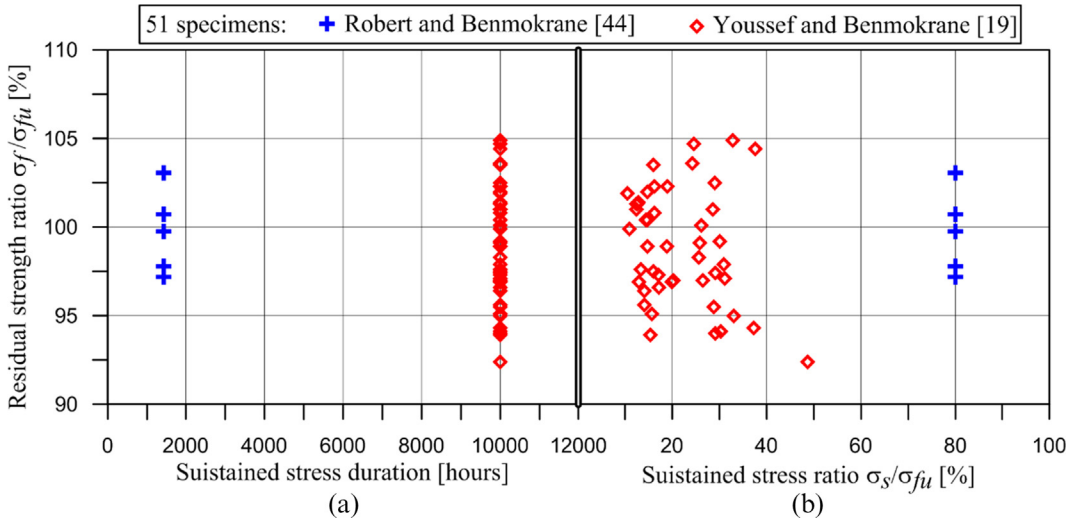

Fig. 2. Residual strength ratio of bars exposed to air (lab conditions) for different a) sustained stress durations and b) sustained stress ratios.

results from other authors for similar exposure conditions and clearly point out the difficulty of comparing results obtained adopting testing (and conditioning) procedures that are markedly different from one another.

3.3. Bars immersed in deionized water

Fifteen specimens were immersed in deionized water and subjected to sustained stress ratios in the range 20%–38%. The deionized water was also heated to accelerate the degradation process. The results, which are shown in Fig. 4a and b in terms of residual strength ratio versus sustained stress duration and sustained stress ratio, respectively, were divided in two groups depending on the temperature of the deionized water, namely 23 °C (3 specimens) and 56–72 °C (12 specimens).

Fig. 4 shows that the sustained load duration had a limited influence on the residual strength ratio of specimens conditioned at 23 °C. In fact, bars conditioned for 10,000 h at 23 °C showed a minimum residual strength ratio σ_f/σ_{fu} = 92.7%. Specimens subjected to high temperatures showed a minimum residual strength

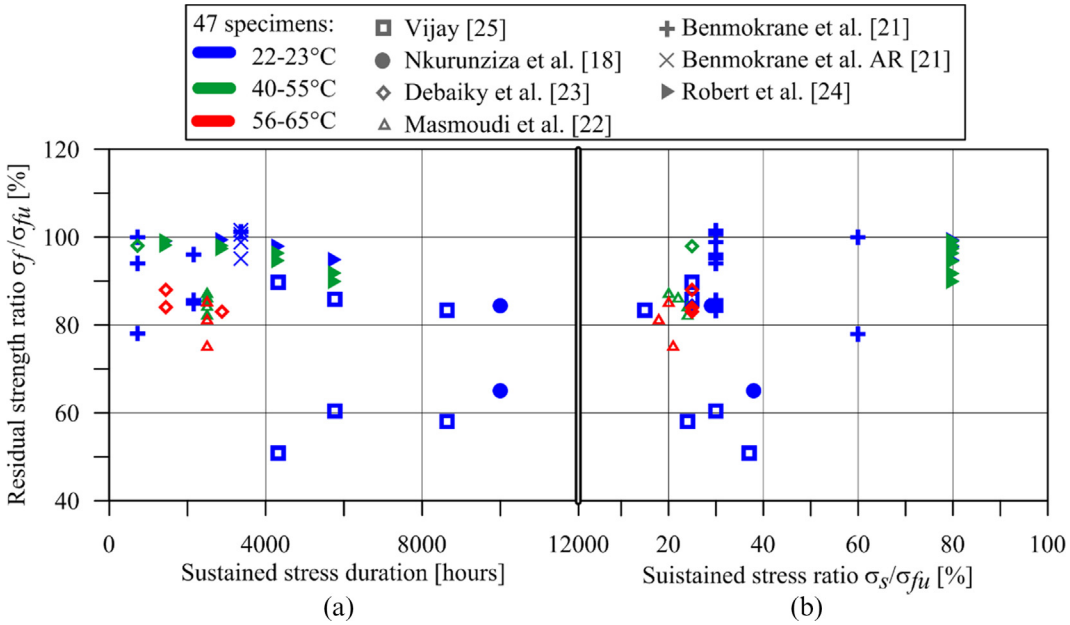

Fig. 3. Residual strength ratio of bars subjected to alkaline environment and sustained stress with respect to sustained stress a) duration and b) ratio.

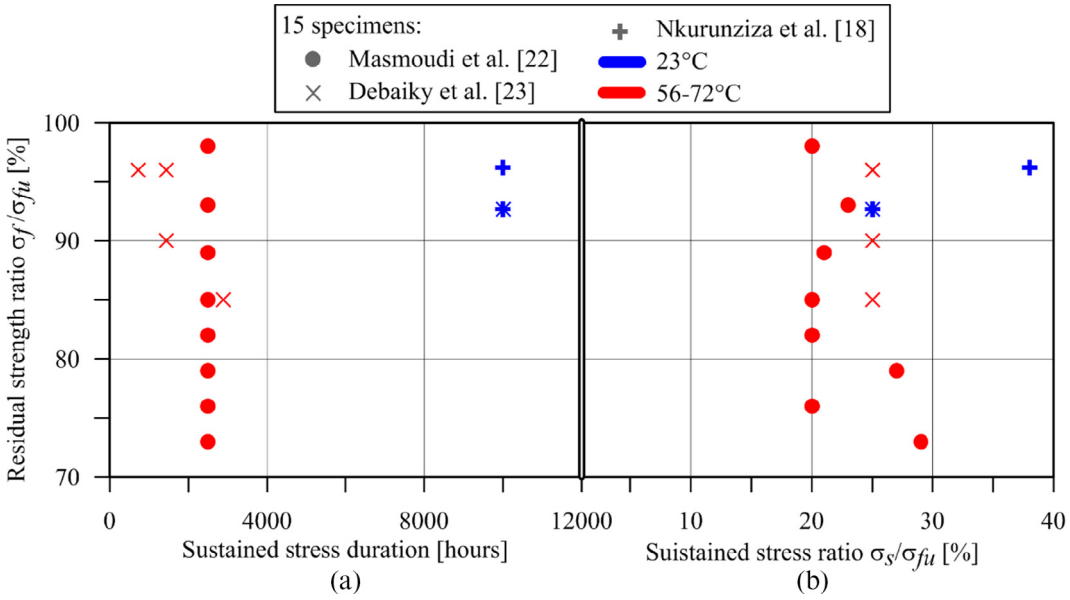

Fig. 4. Residual strength ratio of bars immersed in deionized water and sustained stress with respect to sustained stress a) duration and b) ratio.

ratio σ_f/σ_{fu} = 73% for 2496 h exposure. This result shall be attributed to the high temperature of the deionized water rather than to the sustained stress, as it is clear observing the residual strength ratio σ_f/σ_{fu} = 96.2% obtained from the specimen with σ_s/σ_{fu} = 38% and with a sustained stress duration of 10,000 h.

A clear trend of the residual strength ratio with respect to the sustained stress ratio was not observed (Fig. 4b). Bars tested by Nkurunziza et al. [18] with σ_s/σ_{fu} = 25% and 38% at 23 °C provided similar σ_f/σ_{fu} values (3.6% difference). Results provided by Masmoudi et al. [22] and Debaiky et al. [23] appear scattered and do not allow for observing a clear behavior of σ_f/σ_{fu}. This scatter was attributed to the inherent dispersion of the GFRP bars tensile strength and was considered acceptable by Masmoudi et al. [22], which did not identify a distinct effect of the sustained stress ratios applied (20–29%) due to the additional influence of temperature (57–63 °C) and exposure time.

3.4. Bars immersed in salt solutions

The influence of the sustained load on GFRP bars immersed in salt solution was investigated through tensile tests on 10 conditioned bars (Vijay [25]). The salt solution, which comprised 3% NaCl by weight, were left at room temperature (23 °C) for 6 bars, whereas it was subjected to a total of 141 freeze (−18 °C) – thaw (21 °C) cycles for the remaining 4 specimens. The residual strength ratios obtained are depicted in Fig. 5a and b with respect to the sustained stress duration and ratio, respectively. The results obtained by Vijay [25] showed that the increase of the exposure

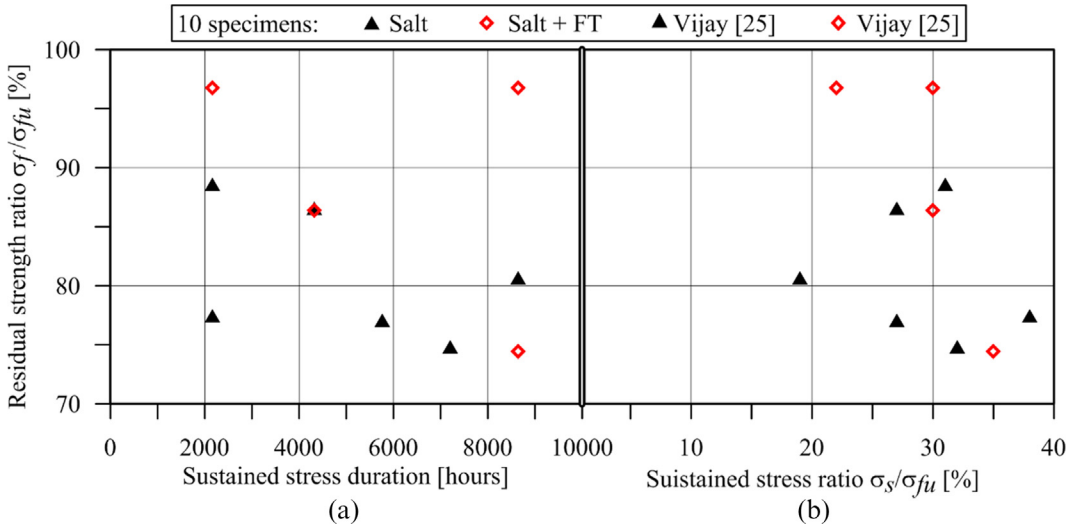

Fig. 5. Residual strength ratio of bars immersed in salt solution and sustained stress with respect to sustained stress a) duration and b) ratio.

time did not significantly affect the bar strength for specimens conditioned at 23 °C. Similarly, specimens subjected to freeze–thaw cycles did not provide a significant strength decrease. The minimum residual strength ratio was σ_f/σ_{fu} = 74.4% for 8640 h exposure time and σ_s/σ_{fu} = 35% (Fig. 5 and Table 1). Nevertheless, one similar specimen conditioned with the same parameters but with σ_s/σ_{fu} = 30% provided σ_f/σ_{fu} = 96.8%. This difference should not be attributed only to the sustained stresses, which values for the two specimens were similar. The limited number of specimens immersed in salt solution does not allow for drawing reliable conclusions on the effect of salt, temperature, and sustained stress. Further tests should be performed to improve our knowledge with respect to these exposure conditions.

3.5. Effect of sustained stress on specimens exposed to alkaline environments

In this section, the effect of sustained stress on GFRP bars exposed to alkaline environments is investigated by comparing the results of specimens conditioned with and without the application of a sustained stress.

The results of 178 tensile tests on bars exposed to alkaline environments without the application of a sustained stress (stress-free), were collected from the literature [25,27,17,28–42]. These bars, some of which were embedded within concrete prism in their central part [34,37], were conditioned in alkaline environments with pH ranging between 12.0 and 13.6 and temperatures between 11 °C and 80 °C. Eight bars made of AR-glass fibers were considered for the analysis [26,40]. Analogously to what was done in Section 3.2, the effect of the different pH values was not investigated whereas specimens were grouped in different temperature ranges, namely range *a* (11–27 °C), *b* (27–55 °C), and *c* (55–80 °C). Details of the stress-free specimens considered with a study of the effect of different pH, exposure temperatures, and fiber volume fractions can be found in Ref. [26].

Fig. 6 shows the comparison between bars exposed to alkaline environment in range *a* (11–27 °C) with (28 specimens) and without (66 specimens) the application of a sustained stress. The residual strength ratios obtained from bars with and without a sustained stress are similar. Assuming that the residual strength ratio is a function of the exposure time only, it was shown that σ_f/σ_{fu} of stress-free bars can be assumed constant with time for a given exposure condition and temperature range [26]. Assuming that this result holds also for stressed bar, the average residual strength ratio $(\sigma_f/\sigma_{fu})_{avg}$ of specimens with sustained stress can be computed without distinguishing between different sustained stress durations. This assumption is furtherly discussed in Section 5. The computed average residual strength ratios of specimens subjected to sustained stress and stress-free are equal to 87.54% (CoV = 0.160, blue dashed line in Fig. 6) and 88.87%

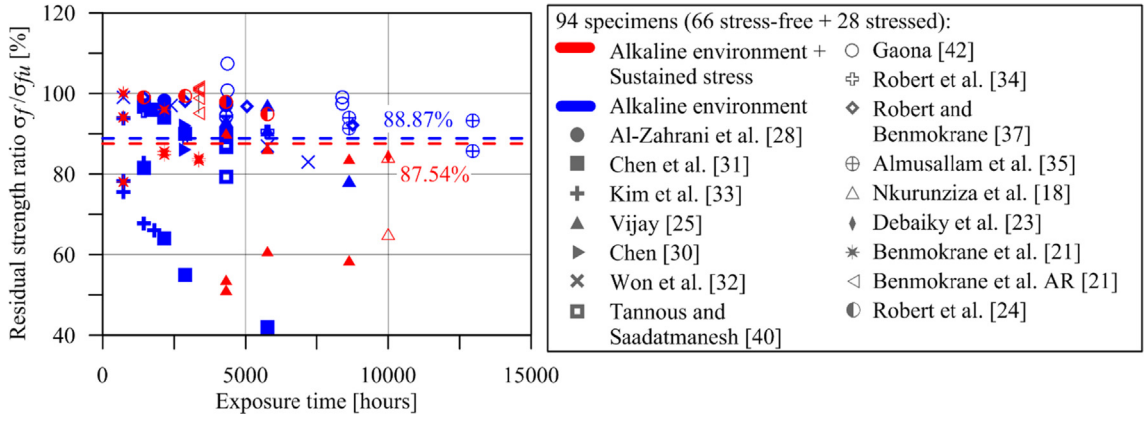

Fig. 6. Comparison between residual strength ratios of bars immersed in alkaline solutions with and without sustained stress at temperatures 11 °C ≤ T ≤ 27 °C.

(CoV = 0.139, red dashed line in Fig. 6), respectively. This small difference suggests that the sustained stress ratio, which ranges between 15% and 80% for specimens in Fig. 6 (see Table 1 and Fig. 3b), has a limited influence on the residual strength ratio.

A comparison between the residual strength ratios obtained from stress-free and stressed specimens in range *b* (27–55 °C) is provided in Fig. 7. Average values $(\sigma_f/\sigma_{fu})_{avg}$, computed assuming no dependence of σ_f/σ_{fu} to exposure time [26], show that also in this case the sustained stress ratio, which ranged between 24% and 80% (see also Table 1 and Fig. 3b), did not adversely affect the residual strength ratio, being $(\sigma_f/\sigma_{fu})_{avg}$ = 84.27% for stress-free bars (CoV = 0.145, blue dashed line in Fig. 7) and $(\sigma_f/\sigma_{fu})_{avg}$ = 92.50% for stressed bars (CoV = 0.066, red dashed line in Fig. 7). However, values of $(\sigma_f/\sigma_{fu})_{avg}$ computed are affected by the different number of stress-free and stressed bars (59 and 13 specimens, respectively) considered.

Results from specimens in range *c* (55–80 °C) are provided in Fig. 8. Similarly to the case of range *b*, specimens in range *c* provided an average residual strength ratio lower for stress-free specimens, i.e. $(\sigma_f/\sigma_{fu})_{avg}$ = 73.15% (CoV = 0.205, blue dashed line in Fig. 8), than for stressed specimens, i.e. $(\sigma_f/\sigma_{fu})_{avg}$ = 82.67% (CoV = 0.053, red dashed line in Fig. 8). However, the number of bars subjected to sustained stress (6 specimens) is significantly lower than that of stress-free bars (53 specimens), which affects the average results obtained. It should be noted that a specimen tested by Sawpan et al. [38] after an exposure time of 17,520 h was not depicted in Fig. 8 but was considered to compute the average residual stress ratio of stress-free bars.

4. Discussion

The experimental results collected allowed for studying the degradation of the tensile strength of GFRP bars simply exposed to air and to different adverse environmental conditions (namely elevated temperature, alkaline environment, deionized water, and salt solution), and subjected to different sustained stress ratios. The results obtained do not show clear trends and the effect of temperature, exposure conditions, and sustained stress, are not always clear.

For most of the tests, long-term conditions were reproduced accelerating the degradation by increasing the environment temperature, which improved (accelerated) the absorption of moisture by the material until reaching the saturation value. Therefore, the bars degradation process was controlled by an artificially-accelerated diffusion rate. However, at temperatures elevated but still below the glass transition temperature of the resin matrix, the physical properties of the bars are modified as a result of the increase of the matrix thermal expansion coefficient [43]. This phenomenon entails for a decrease of the material volume density, which becomes more porous and more permeable to moisture [43].

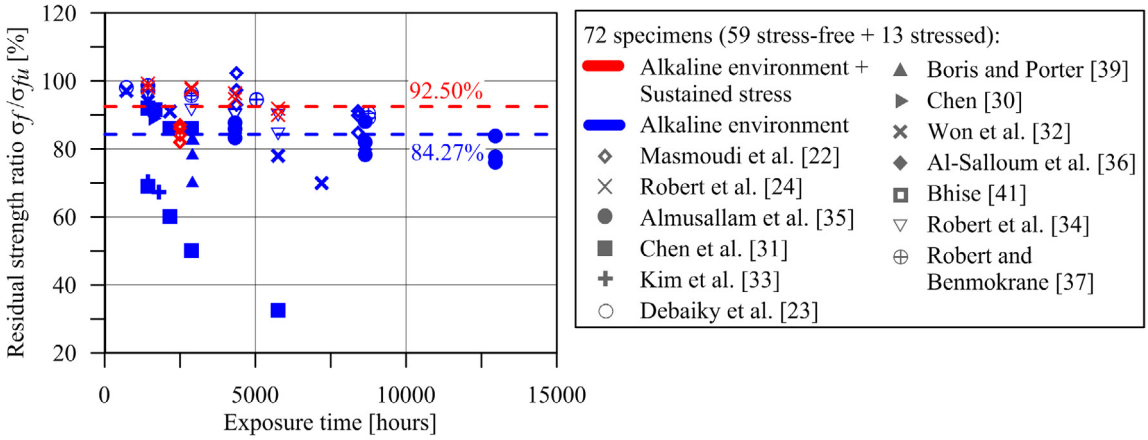

Fig. 7. Comparison between residual strength ratios of bars immersed in alkaline solutions with and without sustained stress at temperatures 27 °C < T ≤ 55 °C.

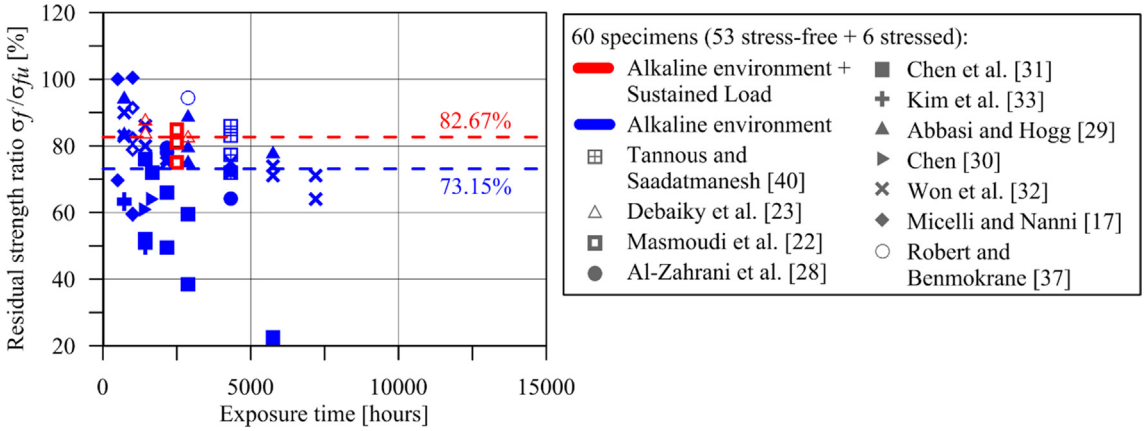

Fig. 8. Comparison between residual strength ratios of bars immersed in alkaline solutions with and without sustained stress at temperatures 55 °C < T ≤ 80 °C.

For accelerated aging tests, it is necessary to select temperatures that do not alter the physical, chemical, and mechanical properties of GFRP bars [26,43]. This alteration may trigger degradation mechanisms different from absorption, resulting in loss of adhesion in the fiber-matrix interface and increased porosity in the material. A range of temperature between −40 °C and +50 °C does not imply alterations in the properties of the bars and is moreover compatible with the climate of regions such as Canada [44] or European countries.

It should be noted that experimental tests are generally carried out by immersion of the specimens in water solutions, whereas in real operating conditions it is difficult to obtain average relative humidity RH values on the bar external surface higher than 90%. This is because GFRP bars are never immersed directly in water as they are embedded within concrete. Investigations in this field confirmed this observation by pointing out that the amount of absorbed moisture for bars immersed in water (RH = 100%) is four times higher than that of an environment with RH = 94% [45]. These considerations suggest that accelerated aging tests may not properly represent the real service conditions, and therefore could highly underestimate the durability of the GFRP bars.

The alkaline environment demonstrated to be the most aggressive for GFRP bars. Comparison of these tests proved to be very complex since many variables affect the test results. Among these variables, those that are of particular importance are the type of bar used (type of fiber, matrix, production process, surface coating, dimension, etc.) and the conditioning methods (temperature, duration, type of solution, pH, etc.).

The damage was found to be remarkable for the bars immersed in alkaline solution, whereas it was of lesser magnitude for specimens embedded within concrete. These results suggest a more detailed analysis of the problem since the alkaline solutions used for the tests should effectively simulate the solution filling the pores of the wet concrete and therefore pH values similar to those characterizing concrete should be expected [26].

Information collected by a research promoted in Canada [46] to verify the conservation status of GFRP reinforcement bars belonging to a real structure subjected to applied loads for more than eight years confirmed the discrepancy between experimental results and natural aging. No loss of adhesion, microcracking, voids formation, and chemical or physical degradation phenomena were observed in the real structure GFRP bars. Such discrepancies are likely to be attributed mainly to the fact that the solution represents a direct and inexhaustible source that can trigger the degradation processes, whereas the volume of the solution in the concrete pores is very small due to the concrete low porosity. Concrete elements are also rarely saturated (generally, the humidity content is 75%-80% of the relative external humidity), as the pores connection is discontinuous and twisted. Therefore, an estimation of the durability of the GFRP reinforcement made on the basis of tests performed on bars immersed in water solution may be not completely reliable.

According to Ref. [18], the behavior of GFRP bars under the effect of permanent load is characterized by three different stages: at high stress (above the "moderate stress" limit) bar breaking occurs due to the progressive failure of the fibers related to excessive sustained stress (creep rupture). At medium stress (between the "low stress" and "moderate stress" limit), the crisis is affected by the penetration of aggressive agents into the matrix cracks caused by mechanical stress (phenomenon of "stress corrosion"). At low stress (below the "low stress" limit), the microstructure of the specimen is not disturbed by the applied stress and good durability is observed even in aggressive environments. The "moderate stress" limit can be set to approximately 45% of the instantaneous tensile strength for a lifetime of 100 years (see for instance [47,48]). The "low stress" limit can be assumed equal to 25–30% of the instantaneous tensile strength (see for instance [21,49]).

The results discussed in this paper do not confirm the existence of three different stages in the behavior of GFRP bars under sustained stress. Furthermore, the stress limits found in the literature appear arguable. To take into account the mutual effects of sustained load and aggressive environments, the American ACI 440.1R-15 [50] and Italian CNR-DT 203/2006 [51] guidelines for design of concrete structures reinforced with FRP bars provide an environmental reduction factor η_a and a long-term effect reduction factor η_l. Combining these two factors at the applied service loads (see Section 5), the stress limits of GFRP bars under sustained stress are $0.14–0.16f_{fu}^{*}$ and $0.21–0.24f_{fk}$ for the American [50] and Italian [51] guidelines, respectively. Similarly, the maximum stress in the GFRP bar under service loads shall be lower than $0.25f_{fu}^{*}$ according to the Canadian standards [52]. The exact value of the stress limit depends on the exposure condition of the reinforced element. f_{fu}^{*} and f_{fk} are the GFRP bar characteristic tensile strength computed by Eqs. (1) and (2), respectively:

$$f_{fu}^{*} = f_{u,avg} - 3\,\bar{s} \tag{1}$$

$$f_{fk} = f_{u,avg} - k \cdot \bar{s} \tag{2}$$

where $f_{u,avg}$ is the mean tensile strength obtained by a sample of specimens, $\bar{s}$ is the associated standard deviation, and k a fractile factor, provided by EN 1990 [53], which depends on the number of specimens in the sample (see Section 5).

According to the proposed limits, the stress induced in the reinforcement by the quasi-permanent service load should be less than approximately 25% of the bar instantaneous strength σ_{fu}, depending on the code/guideline considered. It should be noted that, in general, the maximum stress in the tension steel reinforcement of a reinforced concrete structural element is dictated by the need of guaranteeing the correct functionality of the structure in its ordinary use. In a reinforced concrete beam, such functionality is associated with limited stresses in concrete and in the reinforcement, limited deflection, and control of the crack width. When steel reinforcement is employed, these limits, which are formulated in the Eurocode 2 [54] for the serviceability limit state of RC structures, provide a maximum stress in the reinforcing steel lower than 300 MPa, which is associated with a tensile strain in the steel bar of 0.14%, assuming a steel elastic modulus of 210 GPa. Although 300 MPa is only 36% of a GFRP bar tensile strength assumed equal to 835 MPa, the corresponding strain is significantly higher than 0.14% because the elastic modulus of GFRP bars is usually between 20% and 30% of that of steel bars [50,51]. Therefore, to satisfy the serviceability limit states (i.e. to limit the curvature of a generic cross-section to guarantee the structure functionality, which entails for limiting the tensile strain of the reinforcing bars under the service loads) an amount of GFRP reinforcement higher than that of steel reinforcement is needed, independently of the tensile strength. Studies showed that the amount of GFRP reinforcement often doubles that of the corresponding steel reinforcement for a given service load [55,56]. This means that the stress in the GFRP reinforcement will not exceed 18% of its strength. Since the quasi-permanent load in reinforced concrete beams and slabs is usually not more than 2/3 of the maximum service load, long-term stress in GFRP bars should be lower than 12% of their strength. Therefore, a "low stress limit" equal to 25% of the bar strength does not lead the design process because long-term stresses higher that 25% of the bar strength are meaningless from the design point of view, i.e. in the common practice. This fact should be taken into account to select the sustained stress level for experimental tests and to provide design code/guideline formulations.

Besides all these observations, it should be noted that GFRP manufacturing technology is rapidly improving and current GFRP bars can attain higher strength and better durability performance with respect to bars made with (relatively) old technologies and less quality constituents. New GFRP bars are made of high-quality components (e.g. high performance vinylester resin with low diffusion rate and boron-free glass fibers) and are manufactured using high-standard manufacturing processes and quality control. Therefore, results obtained with new GFRP bars should not be compared with those obtained with old-technology bars.

5. Reduction factors for long-term behavior

The effect of sustained stress on GFRP reinforcing bars is generally considered by employing the design maximum tensile stress σ_{fd} in the serviceability limit state [51]:

$$\sigma_{fd} = \eta_l \eta_a \frac{\sigma_{fk}}{\gamma_m} \tag{3}$$

where η_l and η_a are the long-term effect and environmental reduction factors, respectively, γ_m is the material partial coefficient, and σ_{fk} is the characteristic bar tensile strength. Values of η_a for different exposure conditions were calibrated according to the design by testing procedure provided by EN 1990 [53] using a large database of stress-free GFRP bars. The results obtained showed that η_a can be assumed constant with time for a given temperature and exposure condition [26].

The presence of a sustained stress could potentially increase the degradation induced by an aggressive environment. In general, the effects of sustained load and aggressive environments should not be studied separately and then simply superimposed, but their combined effect should be considered instead. Therefore, the product $\eta_l \cdot \eta_a$ is considered and characteristic and design values of the bar tensile strength are provided applying the design by testing procedure [53] to the results collected in the database described in Section 2.

According to this procedure, the residual strength ratio can be expressed as the product of a normally-distributed unit-mean aleatoric function γ and a deterministic function f:

$$\frac{\sigma_f}{\sigma_{fu}} = \gamma \cdot f\left(t, \xi, \sigma_S/\sigma_{fu}\right) \tag{4}$$

where t is the exposure time and ξ is a parameter related to the exposure conditions. By considering the results collected in the database for a given exposure condition and temperature (or temperature range), the dependency of f on ξ can be eliminated, i.e. $f(t,\xi, \sigma_s/\sigma_{fu}) = f(t, \sigma_s/\sigma_{fu})$. Analyzing the results of bars exposed to air, which is assumed not to affect the bar long-term behavior, it was shown that the bar tensile strength was not influenced by the different sustained stress ratios (Section 3.1), which entails for $f(t, \sigma_s/\sigma_{fu}) = f(t)$. Adopting a linear distribution of the residual strength ratio with respect to the exposure time, the function f can be written as:

$$f(t) = mt + q \tag{5}$$

where m and q are the slope and the y-intercept of the linear distribution f. A linear regression analysis provided the value of m and q, which are reported in Table 2 together with the corresponding coefficient of determination r^2 and number of specimens considered n. Since the slope obtained is very limited ($m = -0.00009$), $f(t)$ was assumed to be constant with t. The y-intercept of the horizontal line, $(\sigma_f/\sigma_{fu})_{avg}$, was computed as:

$$\left(\sigma_f/\sigma_{fu}\right)_{avg} = 1/n \sum_{i=1}^{n} \left(\sigma_f/\sigma_{fu}\right)_i \tag{6}$$

where $(\sigma_f/\sigma_{fu})_i$ is the residual strength ratio of the i-th specimen. $(\sigma_f/\sigma_{fu})_{avg}$ is provided in Table 2 with the indication of the corresponding coefficient of variation (CoV). The small coefficient of variation obtained (CoV = 0.032) indicates a good accuracy of the residual strength ratio estimated.

Once the function f is known, the characteristic (i.e. 5% percentile) and design (i.e. 0.12% percentile) values of the residual strength ratio can be obtained by Eq. (4) by substituting γ with γ_k and γ_d, respectively:

$$\gamma_k = (1 - k_n \cdot \mathrm{CoV}) \tag{7}$$

$$\gamma_d = (1 - k_{d,n} \cdot \mathrm{CoV}) \tag{8}$$

where k_n and $k_{d,n}$ are the characteristic and design fractile factor, respectively, which are provided by EN 1990 [53]. k_n and $k_{d,n}$ varies depending on the number of observations n (i.e. number of tests) and tend to 1.64 and 3.04 for an infinite number of observations. Values of γ_k and γ_d and corresponding values of k_n and $k_{d,n}$ employed are reported in Table 2. $\eta_{1k} \cdot \eta_{ak}$ and $\eta_{1d} \cdot \eta_{ad}$ can be found by combining Eqs. (3) and (4):

$$\eta_{1k} \cdot \eta_{ak} = \gamma_k \cdot f(t) \tag{9}$$

$$\eta_{1d} \cdot \eta_{ad} = \gamma_d \cdot f(t) \tag{10}$$

Setting η_a equal to unity (non-aggressive exposure environment), Eqs. (9) and (10) provide the value of η_{1k} and η_{1d}, respectively. The product $\eta_{1k} \cdot \eta_{ak}$ and $\eta_{1d} \cdot \eta_{ad}$ obtained for bars exposed to air at 23 °C are reported in Table 2.

The coefficient $\eta_{1d} = \eta_{1d} \cdot \eta_{ad} = 0.895$ computed is significantly higher than the corresponding value provided by design guidelines, which is equal to 0.2 and 0.3 for ACI 440.1R-15 [50] and CNR-DT 203/2006 [51], respectively.

The application of a sustained stress and the simultaneous exposure to an aggressive environment could affect the bar residual tensile strength (see Section 4). Applying the design by testing procedure, the simultaneous effect of sustained stress and exposure to aggressive environments can be investigated by analyzing

Table 2
Results of the statistical procedure applied.

Exposure	Range		n	$(\sigma_f/\sigma_{fu})_{avg}$ [%]	CoV	k_n	$k_{d,n}$	γ_k	γ_d	$\eta_{1k} \cdot \eta_{ak}$	$\eta_{1d} \cdot \eta_{ad}$	η_{1d} [26]	m [%/h]	q [%]	r^2
	[°C]	σ_s/σ_{fu} [%]													
Air	23	–	51	98.98	0.032	1.64	3.04	0.948	0.904	0.939	0.895	–	−0.00009	99.83	0.006
Alkaline	22–23	All	28	87.54	0.160	1.67	3.14	0.733	0.498	0.641	0.436	0.666	−0.00231	97.30	0.226
		15–38	22	–	–	–	–	–	–	–	–	–	−0.00247	97.03	0.247
		80	4	–	–	–	–	–	–	–	–	–	−0.00098	101.34	0.777
	40–55	All	13	92.50	0.066	1.71	3.21	0.888	0.789	0.821	0.730	0.610	−0.00062	94.38	0.026
		15–38	5	–	–	–	–	–	–	–	–	–	−0.00746	103.37	0.905
		80	8	–	–	–	–	–	–	–	–	–	−0.00178	102.08	0.857
DI water	22–23	15–38	3	91.10	0.067	1.89	3.56	0.874	0.763	0.796	0.695	0.690	–	–	–
Salt	22–23 + FT	15–38	10	83.95	0.100	1.72	3.23	0.874	0.763	0.695	0.568	0.690	−0.00087	88.65	0.082

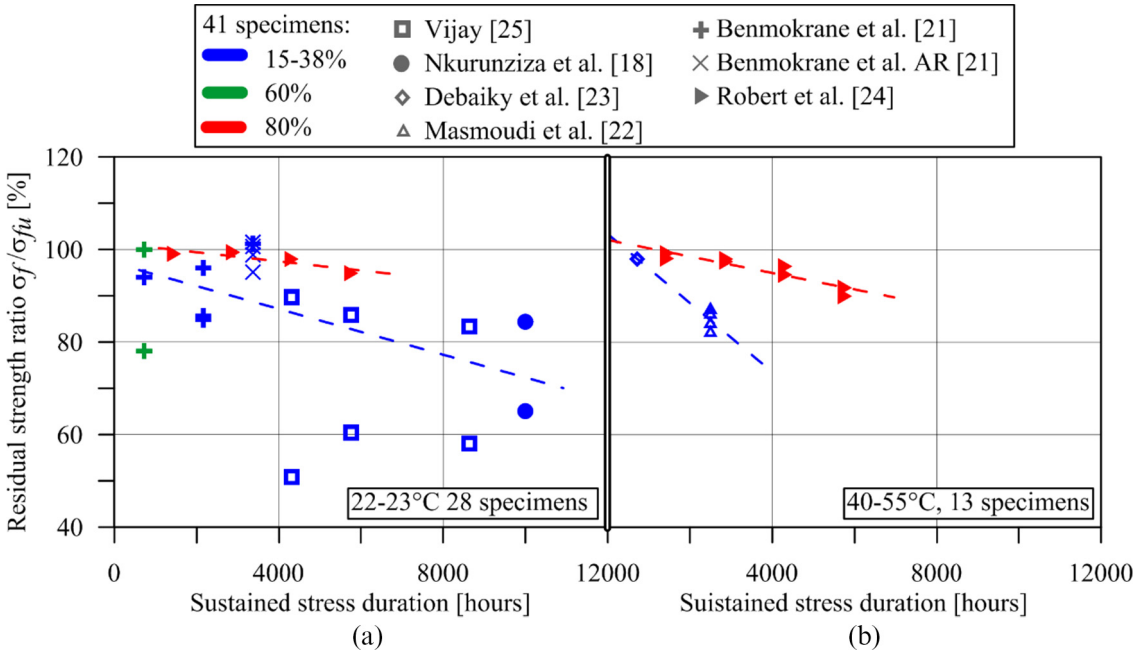

Fig. 9. Fitting of residual strength ratios of bars subjected to alkaline environment for different sustained stress ratio ranges at a) 22–23 °C and b) 40–55 °C.

the results of bars subjected to aggressive environments with different sustained stress ratios, discussed in Section 3. Since high temperatures may affect the degradation processes [26], only specimens conditioned at temperature lower than 55 °C were considered. Specimens were divided in three temperature ranges, namely 22–23 °C, 40–55 °C, and 56–65 °C, and three sustained stress ranges, namely σ_s/σ_{fu} = 15–38%, σ_s/σ_{fu} = 60%, and σ_s/σ_{fu} = 80%. These subdivisions allow for eliminating the dependence of Eq. (4) on ξ and σ_s/σ_{fu}. Considering a linear shape of the residual strength ratio distribution with respect to t, Eq. (5) can be adopted to fit the experimental results. The coefficients m and q obtained by the linear regression analysis of specimens subjected to alkaline environments, immersed in deionized water, and immersed in salt solutions are reported in Table 2, whereas the best fitting lines for specimens subjected to alkaline environments in the range 22–23 °C and 40–55 °C are depicted in Fig. 9a and b, respectively. It should be noted that coefficients for specimens with sustained stress equal to σ_s/σ_{fu} = 60% could not be calibrated because of the limited number of specimens in the database.

Fig. 9 shows that the function f associated with σ_s/σ_{fu} = 80% generally provides higher residual strength ratio than those provided by the function f associated with σ_s/σ_{fu} = 15–38%. This result is in contrast with the assumption that, for a given aggressive environment, the highest level of sustained stress provides the highest bar degradation and suggests that the bar residual strength does not depend on the level of sustained stress. This observation allows for analysing the results without distinguishing between sustained stress level. Therefore, the design by testing procedure was employed to calibrate the product $\eta_l \cdot \eta_a$, which accounts for the combined effect of the specific aggressive environment and sustained stress (range), assuming a linear shape of $f(t,\xi,\sigma_s/\sigma_{fu}) = f(t)$. The coefficients m and q calibrated for all specimens in the specific temperature range subjected to alkaline environments, immersed in deionized water, and immersed in salt solutions are reported in Table 2. Results of specimens immersed in deionized water could not be analysed because all bars were conditioned for the same sustained stress duration. Assuming the slope of f be negligible, as observed for stress-free bars exposed to different aggressive environments [26] and for stressed bars exposed to non-aggressive environments, Eqs. (6)–(8) were employed to compute values of γ_k and γ_d (Table 2). Eqs. (9) and (10) provided the product $\eta_l \cdot \eta_a$ associated to the characteristic and design bar strength, respectively, which characteristic ($\eta_{lk} \cdot \eta_{ak}$) and design ($\eta_{ld} \cdot \eta_{ad}$) values are reported in Table 2 for the different exposure conditions considered. In Table 2, the coefficients η_{1d} computed for stress-free bars subjected to the same exposure conditions studied in this paper [26] are also reported for comparison. In Ref. [26], η_{1d} was not computed for stress-free bars exposed to air and could not be reported in Table 2.

The lowest value, $\eta_{1d} \cdot \eta_{ad}$ = 0.436, was obtained for specimens subjected to alkaline environments at 22–23 °C. This value is lower than η_{1d} = 0.666 computed for stress-free bars subjected to the same exposure conditions [26], which indicates that the application of a sustained stress affected the bar degradation process. However, this result is not confirmed for specimens exposed to 40–55 °C and to specimens immersed in salt water at 22–23 °C and subjected to freeze and thaw cycles, which reported values of $\eta_{1d} \cdot \eta_{ad}$ lower than corresponding values of η_{1d} obtained from stress-free bars (Table 2). $\eta_{1d} \cdot \eta_{ad}$ and η_{1d} were approximately equal for specimens immersed in deionized water.

Although different number of specimens was considered to calibrate $\eta_{1d} \cdot \eta_{ad}$ and η_{1d} (from stress-free bars) for specific environmental exposure and increasing the number of specimen could improve the reliability of the results obtained, the analysis performed suggests that the sustained stress ratio does not play a key role in the residual strength of GFRP bars (except for alkaline environment exposure), confirming results obtained so far from naturally-aged specimens [46].

6. Conclusions

In this paper, the results of 127 tensile tests on stressed GFRP bars exposed to different environmental conditions were collected from the literature and analyzed to provide an insight on the effect of sustained stress on the residual strength of GFRP bars. Although the results are scattered and clear trends could not always be identified, the following conclusions can be drawn:

1. The level of sustained stress ratio appears to have a limited effect on the residual strength ratio obtained.
2. High temperatures have a strong influence on the residual strength ratio of bars exposed to alkaline environments and deionized water, whereas freeze and thaw cycles did not affect the behavior of bars immersed in salt solutions.
3. The comparison between results of specimens exposed to alkaline environments with and without the application of a sustained stress showed that stress-free specimens had the lowest average residual strength ratio for temperature higher than 27 °C. Although the different number of stress-free and stressed tests should be taken into account, this comparison seems to confirm conclusions 1 and 2.
4. Since the elastic modulus of GFRP bars is approximately 25% of that of steel bars, the tensile stress presents in the GFRP bars in a real structure subjected to the quasi-permanent load should be much lower than that in steel bars of an equivalent structure with the same deflection. Consequently, the sustained stress level adopted for experimental tests should not exceed 15% of the tensile strength of the corresponding unconditioned (control) specimen.
5. The design long-term coefficients calibrated confirm that the sustained stress ratio does not play a key role in the bar residual strength except for specimens subjected to alkaline environments.

The results obtained indicate the need of standardized procedures to characterize the long-term behavior of GFRP bars reflecting the real serviceability conditions of GFRP reinforced concrete structures in terms of temperature, exposure conditions, and sustained stress.

Conflict of interest

None.

References

[1] F.G. Carozzi, A. Bellini, T. D'Antino, G. de Felice, F. Focacci, L. Hojdys, L. Laghi, E. Lanoye, F. Micelli, M. Panizza, C. Poggi, Experimental investigation of tensile and bond properties of Carbon-FRCM composites for strengthening masonry elements, Compos. B Eng. 128 (2017) 100–119.

[2] T. D'Antino, T.C. Triantafillou, Accuracy of design-oriented formulation for evaluating the flexural and shear capacities of FRP-strengthened RC beams, Struct. Concr. 17 (3) (2016) 425–442.

[3] T. D'Antino, C. Carloni, L.H. Sneed, C. Pellegrino, Fatigue and post-fatigue behavior of PBO FRCM-concrete joints, Int. J. Fatigue 81 (2015) 91–104.

[4] T. D'Antino, C. Pellegrino, Bond between FRP composites and concrete: assessment of design procedures and analytical models, Compos. B 60 (2014) 440–456.

[5] F. Capani, A. D'Ambrisi, M. De Stefano, F. Focacci, R. Luciano, R. Nudo, R. Penna, Experimental investigation on cyclic response of RC elements repaired by CFRP external reinforcing systems, Compos. B 112 (2017) 290–299.

[6] T. D'Antino, M.A. Pisani, Evaluation of the effectiveness of current guidelines in determining the strength of RC beams retrofitted by means of NSM reinforcement, Compos. Struct. 167 (2017) 166–177.

[7] P. Carrara, D. Ferretti, A finite-difference model with mixed interface laws for shear tests of FRP plates bonded to concrete, Compos. B 54 (2013) 329–342.

[8] C. Bakis, L. Bank, V. Brown, E. Cosenza, J. Davalos, J. Lesko, A. Machida, S.H. Rizkalla, T.C. Triantafillou, Fibre-reinforced polymer composites for construction-state-of-the-art review, ASCE J. Compos. Constr. 6 (2) (2002) 73–87.

[9] S. Pendhari, T. Kant, Y. Desai, Application of polymer composites in civil construction: a general review, Compos. Struct. 84 (2008) 114–124.

[10] A. Mufti, K. Neale, State-of-the-art of FRP and SHM applications in bridge structures in Canada, Compos. Res. J. 2 (2) (2008) 60–69.

[11] G. Fava, M. Bocciarelli, V. Carvelli, M. Pisani, C. Poggi, GFRP bars for internal reinforcement of concrete structures, in: A. Migliacci, P.G. Gambarova, P. Ronca (Eds.), Studies and Researches - Annual Review – Volume 34, RSM, IMREADY srl, Galazzano, 2015, pp. 191–210.

[12] S. Mitchell, The birth of fiberglass boats, Good Old Boat 2 (6) (1999) 23–24.

[13] A.A. Mufti, M. Onofrei, B. Benmokrane, N. Banthia, M. Boulfiza, J.P. Newhook, B. Bakht, G.S. Tadros, P. Brett, Field study of glass-fibre-reinforced polymer durability in concrete, Can. J. Civ. Eng. 34 (3) (2007) 355–366.

[14] I. Daniel, O. Ishai, Engineering Mechanics of Composite Materials, second ed., Oxford University Press, New York, 2006, p. 411.

[15] R. Jones, Mechanics of Composite Materials, second ed., Taylor & Francis, Philadelphia, PA, 1999, p. 506.

[16] R. Pagani, M. Bocciarelli, V. Carvelli, M. Pisani, Modelling high temperature effects on bridge slabs reinforced with GFRP rebars, Eng. Struct. 81 (2014) 318–326.

[17] F. Micelli, A. Nanni, Durability of FRP rods for concrete structures, Constr. Build. Mater. 18 (2004) 491–503.

[18] G. Nkurunziza, B. Benmokrane, A.S. Debaiky, R. Masmoudi, Effect of sustained load and environment on long-term tensile properties of glass fiber reinforced polymer reinforcing bars, ACI Struct. J. 102 (4) (2005) 615–621.

[19] T. Youssef, B. Benmokrane, Creep behaviour and tensile properties of GFRP bars under sustained service loads, in: ACI SP-275, 2011, pp. 39.1–39.20.

[20] M. Robert, B. Benmokrane, Physical, mechanical, and durability characterization of preloaded GFRP reinforcing bars, J. Compos. Constr. 14 (4) (2010) 368–375.

[21] B. Benmokrane, P. Wang, T. Ton-That, H. Rahman, J. Robert, Durability of glass fiber-reinforced polymer reinforcing bar in concrete environment, ASCE J. Compos. Constr. 6 (3) (2002) 143–153.

[22] R. Masmoudi G. Nkurunziza B. Benmokrane P. Cousin, Durability of glass FRP composite bars for concrete structure reinforcement under tensile sustained load in wet and alkaline environments, in: Annual Conference of the Canadian Society for Civil Engineering 2003 Moncton Nouveau-Brunswick, Canada.

[23] A. Debaiky, G. Nkurunziza, B. Benmokrane, P. Cousin, Residual tensile properties of GFRP reinforcing bars after loading in severe environments, ASCE J. Compos. Constr. 10 (5) (2006) 370–380.

[24] M. Robert, P. Cousin, B. Benmokrane, Study of the performance of frp reinforcing bars subjected to extreme conditions of application, Revue Les Annales du Bâtiment et des Travaux Publics 1 (2011) 9–27.

[25] P. Vijay, Aging and design of concrete members reinforced with GFRP bars (PhD Thesis), Department of Civil Engineering, West Virginia University, Morgantown, West Virginia, USA, 1999, p. 205.

[26] T. D'Antino, M.A. Pisani, C. Poggi, Effect of the environment on the performance of GFRP reinforcing bars, Compos. B Eng. 141 (2018) 123–136.

[27] D.K. Stone, D. Koenigsfeld, J. Myers, A. Nanni, Durability of GFRP rods, laminates and sandwich panels subjected to various environmental conditioning, in: Second International Conference on Durability of Fiber Reinforced Polymer (FRP) Composites for Construction, Montreal, Quebec, Canada, 2002.

[28] M.M. Al-Zahrani, S.U. Al-Dulaijan, A. Sharif, M. Maslehuddin, Durability performance of glass fiber reinforced plastic reinforcement in harsh environments, in: The 6th Saudi Engineering Conference, KFUPM, Dhahran, Saudi Arabia, 2002.

[29] A. Abbasi, P.J. Hogg, Temperature and environmental effects on glass fibre rebar: modulus, strength and interfacial bond strength with concrete, Compos. B Eng. 36 (2005) 394–404.

[30] Y. Chen, Accelerated ageing tests and long-term prediction models for durability of FRP bars in concrete (PhD Thesis), Department of Civil and Environmental Engineering, West Virginia University, Morgantown, West Virginia, USA, 2007, p. 214.

[31] Y. Chen, J.F. Davalos, I. Ray, Durability prediction for GFRP reinforcing bars using short-term data of accelerated aging tests, J. Compos. Constr. 10 (4) (2006) 279–286.

[32] J. Won, S. Lee, Y. Kim, C. Jang, S. Lee, The effect of exposure to alkaline solution and water on the strength–porosity relationship of GFRP rebar, Compos. B Eng. 39 (2008) 764–772.

[33] H. Kim, Y. Park, Y. You, C. Moon, Short-term durability test for GFRP rods under various environmental conditions, Compos. Struct. 83 (2008) 37–47.

[34] M. Robert, P. Cousin, B. Benmokrane, Durability of GFRP reinforcing bars embedded in moist concrete, J. Compos. Constr. 13 (2) (2009) 66–73.

[35] T.H. Almusallam, Y.A. Al-Salloum, S.H. Alsayed, S. El-Gamal, M. Aqel, Tensile properties degradation of glass fiber-reinforced polymer bars embedded in concrete under severe laboratory and field environmental conditions, J. Compos. Mater. 47 (4) (2012) 393–407.

[36] Y.A. Al-Salloum, S. El-Gamal, T.H. Almusallam, S.H. Alsayed, M. Aqel, Effect of harsh environmental conditions on the tensile properties of GFRP bars, Compos. B Eng. 45 (2013) 835–844.

[37] M. Robert, B. Benmokrane, Combined effects of saline solution and moist concrete on long-term durability of GFRP reinforcing bars, Constr. Build. Mater. 38 (2013) 274–284.

[38] M.A. Sawpan, A.A. Mamun, P.G. Holdsworth, Long term durability of pultruded polymer composite rebar in concrete environment, Mater. Des. 57 (2014) 616–624.

[39] T. Boris, M. Porter, Advancements in GFRP materials provide improved durability for reinforced concrete, in: Convention, Marketing/technical sessions of the Composites Institute's international composites EXPO '99, Cincinnati, OH, USA, 1999.

[40] F.E. Tannous, H. Saadatmanesh, Durability of AR glass fiber reinforced plastic bars, J. Compos. Constr. 3 (1) (1999) 12–19.

[41] V.S. Bhise, Strength degradation of GFRP bars (PhD Thesis), Department of Civil and Environmental Engineering, Virginia Polytechnic and State University, Blacksburg, Virginia, USA, 2002, p. 105.

[42] F.A. Gaona, Characterization of design parameters for fiber reinforced polymer composite reinforced concrete systems (PhD Thesis), Zachry Department of Civil Engineering, Texas A&M University, College Station, TX, USA, 2003, p. 270.

[43] M. Robert, P. Wang, P. Cousin, B. Benmokrane, Temperature as an accelerating factor for long-term durability testing of FRPs: should there be any limitations?, ASCE J Compos. Constr. 14 (4) (2010) 361–367.
[44] M. Robert, B. Benmokrane, Behavior of GFRP Reinforcing bars subjected to extreme temperatures, ASCE J. Compos. Constr. 14 (4) (2010) 353–360.
[45] A.S.M. Kamal, Towards a better understanding of the mechanism controlling the durability of FRP composites in concrete (PhD Thesis), University of Saskatchewan, Division of Environmental Engineering, Saskatoon, Saskatchewan, 2011, p. 194.
[46] A.A. Mufti, M. Onofrei, B. Benmokrane, N. Banthia, M. Boulfiza, J.P. Newhook, B. Bakht, G. Tadros, P. Brett, Report on the studies of GFRP durability in concrete from field demonstration structures, in: Proceedings of Composites in Construction 2005 - 3rd International Conference, Lyon, France, July 11–13, 2005.
[47] A. Weber, Durability and bond durability of composite rebars, in: CICE 2008, 4th International Conference on FRP Composites in Civil Engineering, 22–24 July, Zurich, Switzerland, 2008.
[48] T. Youssef, S. El-Gamal, E. El-Salakawy, B. Benmokrane, Experimental Results of Sustained Load (Creep) tests on FRP reinforcing bars for concrete structures, in: The 37th CSCE Annual Conference, Quebec City, Quebec, Canada, 2008.
[49] E. Byars, P. Waldron, V. Dejke, S. Demis, S. Heddadin, Durability of FRP in concrete – deterioration mechanisms, Int. J. Mater. Prod. Technol. 19 (1–2) (2003) 28–39.
[50] ACI 440.1R-15, Guide for the Design and Construction of Concrete Reinforced with FRP Bars, American Concrete Institute, Farmington Hills, MI, 2015, p. 88.
[51] CNR-DT 203/2006, Guide for the Design and Construction of Concrete Structures Reinforced with Fiber-Reinforced Polymer Bars, National Research Council, Rome, 2006, p. 35.
[52] CAN/CSA-S806-02, Design and Construction of Building Components with Fibre-Reinforced Polymers, Canadian Standards Association, Rexdale, 2012, p. 198.
[53] European Committee for Standardization (CEN), Eurocode - Basis of Structural Design EN 1990, CEN, Brussels, 2002.
[54] European Committee for Standardization (CEN), Eurocode 2: Design of Concrete Structures - Part 1-1: General Rules and Rules for Buildings EN 1992-1-1, CEN, Brussels, 2004.
[55] V. Carvelli, M. Pisani, C. Poggi, Fatigue behaviour of concrete bridge deck slabs reinforced with GFRP bars, Compos. B Eng. 41 (2010) 560–567.
[56] A. Acciai, A. D'Ambrisi, M. De Stefano, L. Feo, F. Focacci, R. Nudo, Experimental response of FRP reinforced members without transverse reinforcement: Failure modes and design issues, Compos. B 89 (2016) 397–407.